Materials Science in Semiconductor Processing 57 (2017) 178–184

Contents lists available at ScienceDirect

Materials Science in Semiconductor Processing

journal homepage: www.elsevier.com/locate/mssp

Effect of Eu, Mn co-doping on structural, optical and magnetic properties of $BiFeO_3$ nanoparticles

Yiyi Zhu[a], Chuye Quan[a], Yuhui Ma[a], Qi Wang[a], Weiwei Mao[a,b], Xingfu Wang[a,b], Jian Zhang[a], Yonggang Min[a], Jianping Yang[b], Xing'ao Li[a,*], Wei Huang[a,c]

[a] Key Laboratory for Organic Electronics & Information Displays (KLOEID), Synergetic Innovation Center for Organic Electronics and Information Displays (SICOEID), Institute of Advanced Materials (IAM), School of Materials Science and Engineering (SMSE), Nanjing University of Posts and Telecommunications (NUPT), Nanjing 210023, PR China

[b] School of Science, Nanjing University of Posts and Telecommunications (NUPT), Nanjing 210023, PR China

[c] Key Laboratory of Flexible Electronics (KLOFE) & Institute of Advanced Materials (IAM), National Synergistic Innovation Center for Advanced Materials (SICAM), Nanjing Tech University (NanjingTech), 30 South Puzhu Road, Nanjing 211816, PR China

ARTICLE INFO

Keywords:
$BiFeO_3$
Sol-gel method
Multiferroic
Optical
Magnetic properties
Ferroelectric properties

ABSTRACT

Multiferroic $Bi_{1-x}Eu_xFe_{0.975}Mn_{0.025}O_3$ (x=0.025, 0.05, 0.075, 0.1) nanoparticles were prepared by sol-gel route. The impacts of Eu, Mn co-doping samples on the properties of structural, morphology, optical band gap, ferroelectric and ferromagnetic have been systematic investigated. X-ray diffraction and rietveld refinement data reveal that Eu, Mn co-substitution could trigger cubic phase transformation. From the SEM images, the grains of all the samples are asymmetrical and anomalous in shape and interestingly, the particle size of the samples decrease from 200 to 500 nm to ~100 nm after doping. And we can obtain the content of dopants in the samples by energy-dispersive X-ray spectroscopy (EDS) analysis. UV–vis absorption spectra demonstrate a gradually decreasing of the direct optical band gap from 2.40 eV to ~1.49 eV with doping Eu and Mn in BFO. X-ray photoelectron spectroscopy (XPS) analyses illuminate that Eu, Mn-doping results in the increase of Fe^{3+} ions content in the samples. The significantly increased the remanent magnetization (M_r) and coercive field (E_c) were caused by Eu and Mn co-doping.

1. Introduction

During the last few decades, much attention has been paid to multiferroic materials because of their rich physical properties and potential application in memory devices [1–3]. Multiferroics, which simultaneously exhibits ferroelectric, magnetic and magnetoelectric properties, have attracted huge research enthusiasm in single phase materials [4]. Among the multiferroic materials researched, so much focus is given to the perovskite bismuth ferrite $BiFeO_3$ (BFO) which displays G-type antiferromagnetism and ferroelectricity, and have a high Neel temperature (T_N~643 K) and Curie temperature (Tc~1103 K) [5,6]. Though it has the unique properties, there are some inherent disadvantages of pure BFO such as antiferromagnetic nature and high conductivity due to its charge defects [7]. Besides, the weak magnetoelectricity from spatial periodic inhomogeneous spin structure could restrict the applications in high density memory, photovoltaic and electromechanical devices [8]. There are many groups which have studied the optical, ferroelectric and magnetic characteristics of BFO nanomaterials [9–13].

Various efforts have been devoted to solving the drawbacks such as rare-earth element or/and transition metal doping [9,12,14,15]. For instance, modifying the Bi-site by rare-earth elements (Eu [17], Tb [18], Sm [9], etc) to enhance ferroelectric polarization and dielectric constant have been reported. Also accompany the regional doping of Fe-site by Mn, Sc and Ca ions can obviously effect on destruction of the spin cycloid to promote its multiferroic properties [6,16,19]. So the co-doping is a good choice for us to gain BFO with excellent characters. And up to now a few investigations focusing on the Eu and Mn co-doped BFO.

In this study, a series of $Bi_{1-x}Eu_xFe_{0.975}Mn_{0.025}O_3$ (x=0.025, 0.05, 0.075, 0.1) nanoparticles were fabricated by sol-gel methods. The microstructure, ferroelectric and magnetic characteristics of BFO and Eu, Mn co-doped BFO are discussed in detail.

* Correspnding author at: Key Laboratory of Flexible Electronics (KLOFE) & Institute of Advanced Materials (IAM), National Synergistic Innovation Center for Advanced Materials (SICAM), Nanjing Tech University (NanjingTech), 30 South Puzhu Road, Nanjing 211816, PR China.

E-mail addresses: lxahbmy@126.com (X. Li), iamwhuang@njupt.edu.cn (W. Huang).

http://dx.doi.org/10.1016/j.mssp.2016.10.023
Received 19 June 2016; Received in revised form 15 October 2016; Accepted 17 October 2016
Available online 24 October 2016

2. Experimental

The polycrystalline anoparticles of $Bi_{0.975}Eu_{0.025}Fe_{0.0975}Mn_{0.025}O_3$, $Bi_{0.95}Eu_{0.05}Fe_{0.0975}Mn_{0.025}O_3$, $Bi_{0.925}Eu_{0.075}Fe_{0.0975}Mn_{0.025}O_3$ and $Bi_{0.9}Eu_{0.1}Fe_{0.0975}Mn_{0.025}O_3$ (named BEFM1, BEFM2, BEFM3 and BEFM4, respectively) were prepared by sol-gel route. In order to gain high quality samples, we used high pure (99.99%) Bi_2O_3, $Fe(NO_3)_3{\cdot}9H_2O$, Eu_2O_3 and MnO as starting materials. These materials with proper stoichiometric proportions were dissolved in HNO_3 and tartaric acid was mixed as complexing agent. The resultant liquor was placed on a hot slab with constant magnetic stirring for 2 h at 50 ℃ to acquire sol and then the sample was dehydrated at 70 ℃ for 24 h. Finally, the powder was put into tube furnace at 550 ℃ for 2 h to get $Bi_{1-x}Eu_xFe_{0.975}Mn_{0.025}O_3$ with high crystalline.

By a set of characterization means, the finished powders were searched and analyzed. The composition of the BEFM nanocrystals was determined by X-ray diffractometer (XRD). By performing the scanning electron microscope (SEM), we can know the microstructure, average particle size and morphology of the samples. The Violet–visible absorption spectra values were investigated by PerkinElmer Lambda 35 ultra violet-visible photometer. The valence states of Fe ions in the nanoparticles were performed by X-ray photoelectron spectroscopy (XPS, ESCALAB 250Xi). To study the ferroelectric characters, samples were carried out using Radiant accuracy materials analyzer. Before the study, all powders was translated into a slice of size 0.5 cm in diameter and about 0.06 cm in thickness. The silver electrodes were directly coated on the surface. Magnetic were obtained via the Magnetic Property Measurement System.

3. Results and discussion

We utilize the powder XRD technique to analyze the crystal structures of the undoped BFO, BEFM1, BEFM2, BEFM3 and BEFM4 nanoparticles. From Fig. 1, the main characteristic peaks of the samples (~32°2θ) are well crystallinity and pure polycrystalline compared with Eu, Mn co-doped film [20]. The XRD pattern of BFO shows the distorted rhombohedral crystal structure, which the standard crystal data corresponding to the JCPDS Card (71-2494) are retrieved. As more Eu ions are added, the remarkable changes in the diffraction patterns are the merging of the doubly split peaks (104)/(110) compared with the pristine sample, as seen in Fig. 1(b). The merged peak indicates that the structural transformation occurred after doping. The behavior of the two peaks gradually combined with broader and shifts to the higher degree values can attribute to the significantly change in interplanar spacing and the grain size [18] induced by Eu and Mn co-doping.

To further investigate the structure transformation, it is necessary to further explore the XRD data. So we implemented Rietveld refinement of XRD patterns by employing FullProf software. According to the observation and calculation, Fig. 2 reveals the different refined XRD patterns of all the samples. From the refinement results, the

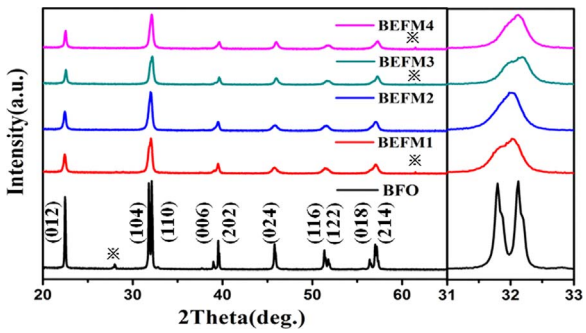

Fig. 1. (a) X-ray diffraction (b) Enlarged XRD patterns of all the samples. (The asterisks "※" mark the negligible impurity phase)..

coexistence of rhombohedral and cubic crystal system is observed. The crystal structure parameters, GOF-index and profile R-factors come from the FullProf are listed in Table 1. Small goodness of fitting (GOF) and R-values of refinements (R_p, R_{wp} and R_e) mean that the simulated parameters can fit the measured data of XRD patterns very well [21]. From Table 1, we can see that the BEFM1 has two main phase namely rhombohedral *R3c* (94.04%) and cubic PM-3M (5.96%). But in the BEFM4, we found the content of cubic phase is as high as 52.28%. This illustrates the doping of Eu leads to a change of crystal structure and the enhancement of cubic phase on ferroelectric and magnetic properties have been reported [23,24]. Structural phase transition can be explained by the Goldschmidt tolerance factor (t) which predict the structural stability of a perovskite-related oxide [25].

$$t = \frac{r_A + r_B}{\sqrt{2}(r_B + r_O)} \quad (1)$$

where r_A, r_B, and r_O are the ionic radii of Bi-site, Fe-site, and O-site ions, respectively. Compared with Bi^{3+}(1.17 Å), the ionic radius of Eu^{3+}(1.07 Å) is smaller, so the tolerance factor of BFO decrease after replacing. This indicates that the stability of perovskite phase became worse [25]. In addition, bond length of Bi/Fe-O and the bond angle of Fe-O-Fe are found to have a close relation with the ferromagnetic natures [26]. The average bond distance together with the bond angle calculated are listed in Table 2.

Scanning electron microscopy technology was used in pure and co-doped BFO powders on the conducting resin, as shown in Fig. 3. Obviously, all the samples show distinct morphologies and clear boundaries morphology. With the increase of Eu and Mn content, the particle size decreases from 200 to 500 nm to ~ 100 nm. Grain size reduction means the co-doping can suppress the growth of the grain. Doping rare earth and transition metal elements in BFO which can affect the growth of the grains is also common in other elements doped BFO particles [27] and ceramics [17,28]. The reduce of the granule size in the co-doped powders may be analyzed from three aspects (i) The partial substitution Bi-site by Eu and Fe-site by Mn may lead to the inhibition of oxygen vacancy amount, which bring about tardiness oxygen ion motion and then the growth rate of grain lower [22]. (ii) The Eu and Mn may act as nucleating agent. Thus, with the increase in nucleation rate, the grain growth rate is limited obviously [29]. (iii) Because of the different diffusion rates of components, Kirkendall effect may be the another reason [30]. In order to confirm the content of dopants in BFO and BEFM samples, the energy-dispersive X-ray spectroscopy (EDS) are shown in Fig. 4. The EDS data of the BEFM samples indicate that the atomic ratio of Eu to Mn are approximately 1.088:1, 1.879:1, 3.069:1 and 4.103:1 respectively.

The UV–Visible absorption spectra of as-prepared samples are shown in Fig. 5(a). It is clear that all the samples display one absorption peaks between 450 and 550 nm, which indicates a blue-shift as the content of Eu increases. As we can see the absorption bands of the samples are around 500 nm, which means electronic transitions between conduction-band Fe 3d states and valence-band O 2p states. So the reason for excursion in the absorption edges is that the change in electronic structure of samples. As we all know, the energy band gap (Eg) plays a key role in the semiconductor of BFO, which can be calculated with the assist of absorption spectra (Fig. 5(a)). And for direct band gap semiconductor, the Eg can be counted via classical Tauc's law [31]:

$$\alpha h\nu = A(h\nu - Eg)^{1/2}$$

where h is Planck's constant, α and hν are the absorption coefficient and incident photon energy, A is a constant function. The graph of $(\alpha h\nu)^2$ against hν for the samples are shown in Fig. 5(b). And we ensure the Eg value by extending the straight line section of $(\alpha h\nu)^2$ to zero, as seen in Fig. 5(b). To get a better look at the change of Eg, we plotted the Eg versus Eu content with the illustration of Fig. 5(b). Obviously, the Eg decreased gradually from 2.40 eV [32] to about 1.49 eV after doping